P. Dewallef
ASMA Department, University of Liège, 1 Chemin des Chevreuils, 4000 Liège, Belgium
e-mail: p.dewallef@ulg.ac.be

C. Romessis
Laboratory of Thermal Turbomachines, National Technical University of Athens, P. O. Box 64069, Athens 15710, Greece
e-mail: cristo@mail.ntua.gr

O. Léonard
ASMA Department, University of Liège, 1 Chemin des Chevreuils, 4000 Liège, Belgium
e-mail: o.Leonard@ulg.ac.be

K. Mathioudakis
Laboratory of Thermal Turbomachines, National Technical University of Athens, P. O. BOX 64069, Athens 15710, Greece
e-mail: kmathiou@central.ntua.gr

Combining Classification Techniques With Kalman Filters for Aircraft Engine Diagnostics

A diagnostic method consisting of a combination of Kalman filters and Bayesian Belief Network (BBN) is presented. A soft-constrained Kalman filter uses a priori information derived by a BBN at each time step, to derive estimations of the unknown health parameters. The resulting algorithm has improved identification capability in comparison to the stand-alone Kalman filter. The paper focuses on a way of combining the information produced by the BBN with the Kalman filter. An extensive set of fault cases is used to test the method on a typical civil turbofan layout. The effectiveness of the method is thus demonstrated, and its advantages over individual constituent methods are presented. [DOI: 10.1115/1.2056507]

Introduction

Diagnostic methods employing statistical inference can be mainly categorized into *regression methods* and *classification methods*, depending on the way information is processed. In classification problems the task is to assign an input to one of a number of discrete classes or categories. However, in regression problems the outputs represent the values of continuous variables [1]. For example, in the case of aircraft engine diagnostics, outputs of the regression algorithm is a set of numerical health parameter values, whereas for a classification algorithm each parameter is assigned to a given class ("faulty not faulty" or "low correct high").

Applying regression techniques such as Kalman filtering on gas turbine engine diagnosis [2,3] poses some stability problems when few measurements are available; health parameter estimation is unstable when a low redundancy is encountered. Indeed, for commercial aircraft engines (twin spool high bypass ratio turbofan engines), it is typical to have more than 10 parameters to estimate from only seven to nine measurements. As a result of the negative redundancy, the problem is underdetermined and the solution is not unique. Moreover, this estimation relies on uncertain observations available under the form of a noisy measurement set. Increasing the number of samples could make the redundancy positive, but because they are related to nearly the same operating points they do not represent a set of independent observations, and therefore, the estimation remains unstable. Some approaches in turbine engine diagnostics where few measurements are available in [4–8], but they all assume some predefined configurations for the faults. Those predefined configurations are built into the algorithm, and it is not possible for the user to interact with them.

As stated above besides regression algorithms, classification algorithms solve the same problem in a different way and, therefore, give a different kind of results. Although less accurate, classification algorithms are more reliable and usually more stable. Moreover, some classification algorithms allow some qualitative knowledge (i.e., user experience, some events that have been observed but cannot be modeled, etc.) to be introduced into the classification rule. Those characteristics make classification algorithms very complementary to regression algorithms. Some results of classification techniques applied to turbine engine diagnostic can be found in [9,10].

In [11], a physical state variable model is combined with a neural network model to improve the diagnostic of a turbine engine by including empirical knowledge. Although the present contribution uses a different method, the final scope is the same: to decrease the proportion of false alarms and to increase the proportion of fault detection by taking advantage of two different kind of methods.

The approach presented in this contribution is based on a soft-constrained Kalman filter (SCKF) developed in [8] and a Bayesian Belief Network (BBN) developed in [9]. The principal diagnostic tool is the Kalman filter, which produces the estimations of the unknown health parameters. The estimation process incorporates information derived by the BBN—a fact that is shown to improve fault detection efficiency. A way of combining the two techniques is described in the following. For completeness, a brief description of the diagnostic problem and the structure of each of the two techniques is given first.

Problem Statement

The identification problem consists of recursively estimating a set of health parameters representing possible degradations of specific components (fan, high pressure turbine, etc.) on the basis of successive measurement samples performed on a turbine engine. A steady-state model of this engine must be made available for measurement simulation. This model is based on a set of health parameters $\mathbf{w}_k$, engine operating point $\mathbf{x}_k$, and command parameters $\mathbf{u}_k$. The set of predicted measurement $\hat{\mathbf{y}}_k$ is generated through this nonlinear model $\mathcal{G}$

$$\hat{\mathbf{y}}_k = \mathcal{G}(\mathbf{u}_k, \mathbf{x}_k, \mathbf{w}_k) \tag{1}$$

Health parameter identification is intended to solve the inverse problem of measurement prediction: inputs are the raw measurements $\bar{\mathbf{y}}_k$ and outputs are the health parameters $\hat{\mathbf{w}}_k$ to be estimated. The process starts with initial values for the health parameters $\hat{\mathbf{w}}_k$. Residuals are built as $\bar{\mathbf{r}}_k = \bar{\mathbf{y}}_k - \hat{\mathbf{y}}_k$ to compare predicted measurements $\hat{\mathbf{y}}_k$ to observed measurements $\bar{\mathbf{y}}_k$. Although classification

Contributed by the International Gas Turbine Institute (IGTI) of The American Society of Mechanical Engineers for publication in the ASME Journal of Engineering for Gas Turbines and Power. Paper presented at the International Gas Turbine and Aeroengine Congress and Exhibition, Vienna, Austria, June 13-17, 2004, Paper No. GT2004-53541. Manuscript received by IGTI, October 1, 2003; final revision, March 1, 2004. IGTI Review Chair: A. J. Strazisar.

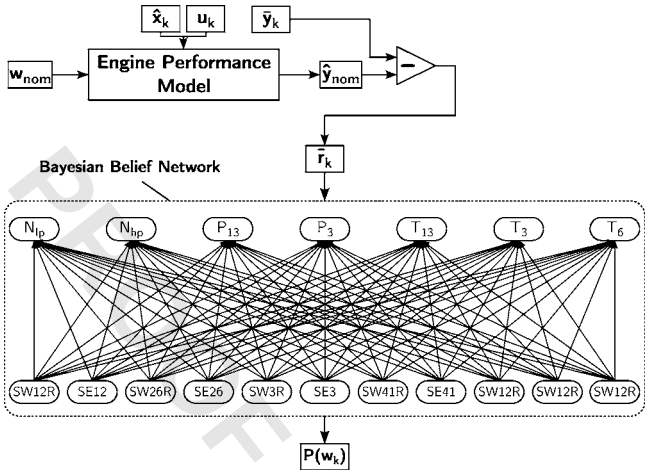

Fig. 1 Classification procedure using BBN

algorithms are aimed at associating a given class to each residuals $\bar{\mathbf{r}}_k$, the purpose of regression algorithm is to fit health parameters to observed raw measurements $\bar{\mathbf{y}}_k$ and leads to drive residuals $\bar{\mathbf{r}}_k$ to zero. Regression problems are thus solved through the minimization of the following inner product, which is also known as the weighted least-squares approach where the weighting factor $\mathbf{R}_r$ is the residual covariance

$$\mathcal{J} = \bar{\mathbf{r}}_k^T \mathbf{R}_r^{-1} \bar{\mathbf{r}}_k \tag{2}$$

Classification Techniques: BBN

The classification technique is a Bayesian Belief Network (BBN), presented in [9] (to which the interested reader is referred for more details). The structure of such a network, which will be employed later in the paper, is shown in Fig. 1. It includes 18 nodes representing deviations of 11 health parameters ($\hat{\mathbf{w}}_k$), and seven measurements ($\bar{\mathbf{y}}_k$) for the test case of a turbofan engine.

The BBN is supported by an engine performance model. A set of measurement readings ($\bar{\mathbf{y}}_k$) is preprocessed together with $\hat{\mathbf{x}}_k$ and $\mathbf{u}_k$ to derive the deviation of the seven measurements from their nominal value. These deviations are presented to the BBN, from which the output probabilities $P(\mathbf{w}_k)$ are estimated. Each output node produces the probability for a health parameter to belong to a certain interval, for example, to be around the value that represents a "healthy" component or to be away from this value for a fault condition. The output is thus an indication of what the most probable values of health parameters are, and from this information the stand-alone BBN derives a fault diagnosis.

Soft-Constrained Kalman Filters

The soft-constrained Kalman filter (SFKF) has a typical structure depicted in Fig. 2. Details on the specific SCKF employed here can be found in [8], where the development of this filter is

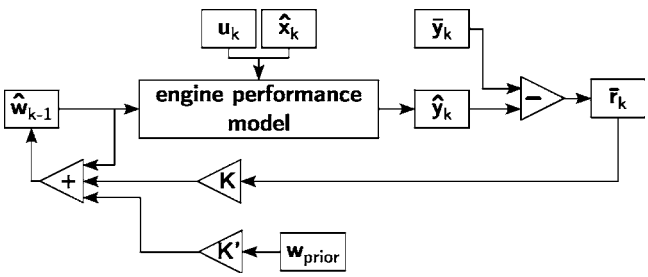

Fig. 2 Description of the soft-constrained Kalman filter

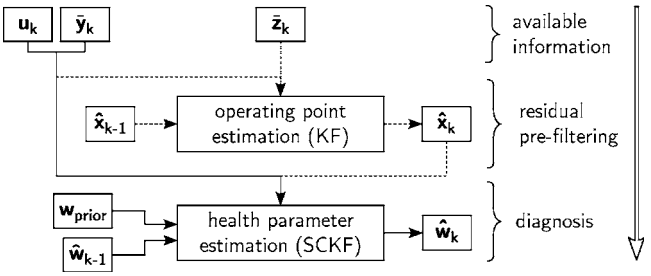

Fig. 3 Data preprocessing for operating-point estimation

described. A Kalman filter is a regression algorithm, meaning that its outputs are numerical values of health parameters. Differences between regression methods found in the literature reside in the update rule selected to minimize $\mathcal{J}$ regarding $\hat{\mathbf{w}}_k$. Many methods found in the aircraft-engine diagnostic literature are *batch* methods where the whole set of available data is processed in one batch. In the case of non-linear engine performance model such an estimation involves the use of non-linear iterative optimization methods and the estimation is therefore called *batch iterative*. At the other hand, *recursive* procedures do not involve the batch processing of the full block of data but only a simple update of the parameters each time new data are available. Moreover, the updating scheme does not imply any optimization procedure. Generally speaking, the advantage of a recursive approach resides in the quick and simple update formula provided by those algorithms that is well suited for on-line estimation.

As outlined in Fig. 2, prior information is introduced into the identification loop. This is done through a penalizing term added to the objective function and favoring health parameters, which are in the neighborhood of predetermined values $\mathbf{w}_{\text{prior}}$. This process is called *ridge regression* [12,13]. Because this prior information is assumed to be Gaussian, it is parametrized by its mean $\mathbf{w}_{\text{prior}}$ and covariance matrix $\mathbf{D}$. Prior information on health parameters are assumed to be uncorrelated, and $\mathbf{D}$ is thus strictly diagonal. $\hat{\mathbf{w}}_{k-1}$ is updated by combining $\mathbf{w}_{\text{prior}}$ to current raw measurements $\bar{\mathbf{y}}_k$ to assess $\hat{\mathbf{w}}_k$. It is through $\mathbf{w}_{\text{prior}}$ that coupling the BBN is achieved, as explained in the next section.

In Fig. 2, the engine operating point $\mathbf{x}_k$ is assumed to be known. In this contribution it is estimated using a Kalman filter together with an additional measurement set $\bar{\mathbf{z}}_k$. The complete sequence is described in Fig. 3. A set of measurements together with the set of command parameters are preprocessed into a Kalman filter that estimates the operating point $\hat{\mathbf{x}}_k$, which is used afterward in the health-parameter estimation.

Combining Classification Techniques to Kalman Filters

The flowchart of the procedure combining the Kalman filter and BBN is summarized in Fig. 4. Both the BBN and Kalman filter

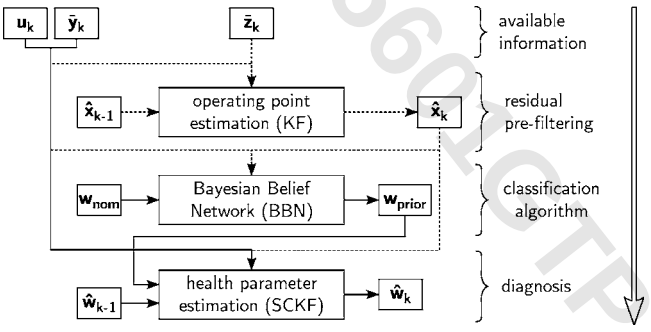

Fig. 4 Procedure followed to combine classification algorithm with Kalman filter

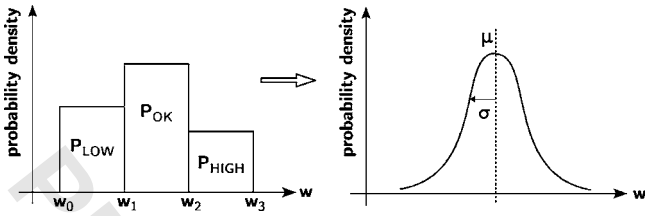

Fig. 5 Conversion of probability density from a piecewise constant function into a Gaussian function

use the same preprocessing through operating-point estimation. It increases the measurement prediction accuracy for both algorithms. BBN results are fed into the SCKF as prior information to achieve the health-parameter estimation. The final outcome of the combination is the SCKF result called hereafter "results of the combination."

The communication between a classification algorithm, such as the BBN, and a Kalman filter is not straightforward because they use different probability density functions. Although prior information needed by the Kalman filter has to be Gaussian, outputs of classification algorithms are the probabilities of a measurement set to belong to a specific class and, therefore, no probability density function is attached to the results. This situation is depicted in Fig. 5. Probabilities related to outputs of the classification algorithm are assumed to be piecewise constant and must be converted into a Gaussian one to be fed into the SCKF.

The problem of Fig. 5 underlines the more general situation where qualitative knowledge is to be compared to quantitative knowledge. This difference in usually sufficient to prevent the combination between classification techniques and regression techniques. The solution proposed herein is to preserve, as much as possible, the distribution of probability given by the BBN. If the BBN diagnoses that a given parameter belongs to a specific fault case with a probability of 100%, then this must appear in the Gaussian function fed into the Kalman filter by a small covariance. Conversely, if the BBN is unable to make a diagnostic, then the probability is spread on the whole set of possible categories; this must also appear in the Gaussian function fed into the Kalman filter by an important variance. The most efficient way to translate this knowledge is to go back to the definition of the mean μ and the variance σ^2 of a given probability function p

$$\mu = \int_{-\infty}^{\infty} wp(w)dw \tag{3}$$

$$\sigma^2 = \int_{-\infty}^{\infty} (w-\mu)^2 p(w)dw \tag{4}$$

Applying relations (3) and (4) to the situation in Fig. 5 yields

$$\mu = \sum_{i=0}^{n_c} \int_{w_i}^{W_{i+1}} w \frac{P_i}{w_{i+1}-w_i} dw = \sum_{i=0}^{n_c} \frac{P_i}{2}(w_i + w_{i+1}) \tag{5}$$

$$\sigma^2 = \sum_{i=0}^{n_c} \int_{w_i}^{W_{i+1}} (w-\mu)^2 \frac{P_i}{w_{i+1}-w_i} dw = \sum_{i=0}^{n_c} \frac{P_i}{3}[(w_i-\mu)^2 + (w_i-\mu)^2 + (w_i-\mu)(w_{i+1}-\mu)] \tag{6}$$

The mean and covariance needed by the Kalman filter are, respectively, built using relations (5) and (6). These are the key relations that allow the flow of information from BBN to SCKF.

Application of the Method

In order to show how the method achieves a diagnosis and "examine" its effectiveness, its application to a test case of a twin-spool mixed-flow turbofan is presented. This type of engine is representative of current-day civil aircraft propulsors. The particular engine layout chosen is shown in Fig. 6. This engine and fault cases examined has been used as a test case by several previously published diagnostic methods (e.g., [5,7–9]). It can therefore be considered as a benchmark case. The available sensors with their accuracies and the set of 11 health parameters representing some degradations of specific components (fan, high pressure turbine, etc.) are shown in Fig. 6.

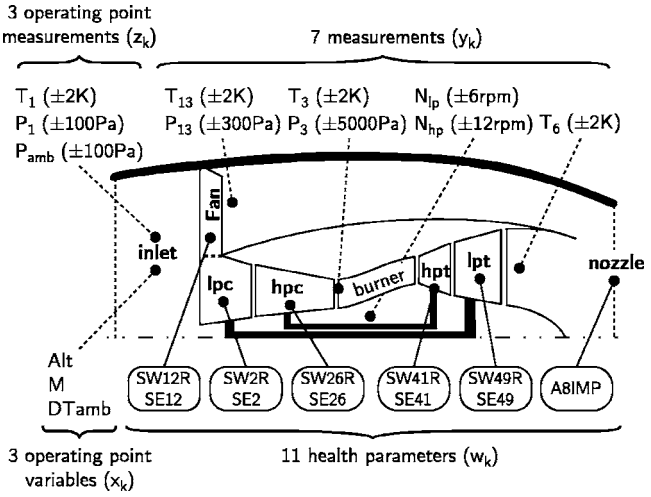

Fig. 6 Turbofan engine layout. Measurement uncertainties represent three times the standard deviation

An extensive set of faults, shown in Table 2, representative of possible situations expected to be encountered in practice, defined

Table 1 Detailed nomenclature of Fig. 6

ALT=flight altitude
DTAMB=ΔT from iso
M=flight Mach number
Tx=total temperature at station *x*
Px=total pressure at station *x*
SEx=efficiency degradation at component *x*
SWxR=flow capacity at component *x*
A8IMP=fouling factor of the nozzle
LPC=low-pressure compressor
HPC=high-pressure compressor
HPT=high-pressure turbine
LPT=low-pressure turbine

Table 2 Fault cases of a turbofan engine

a	−0.7% on SW2R	−0.4% on SE2	FAN, LPC
	−1% on SW12R	−0.5% on SE12	
b	−1% on SE12		
c	−1% on SW26R	−0.7% on SE26	HPC
d	−1% on SE26		
e	−1% on SW26R		
f	+1% on SW42R		HPT
g	−1% on SW42R	−1% on SE42	
h	−1% on SE42		
i	−1% on SE49		LPT
j	−1% on SW49R	−0.4% on SE49	
k	−1% on SW49R		
l	+1% on SW49R	−0.6% on SE49	
m	+1% on A8IMP		Nozzle
n	−1% on A8IMP		
o	+2% on A8IMP		

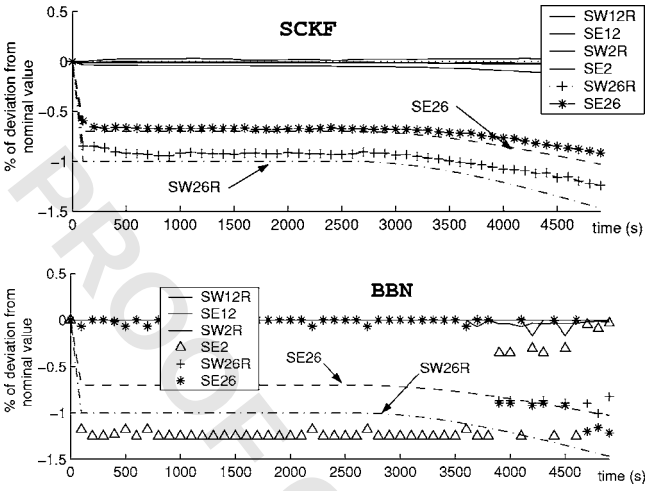

Fig. 7 Identification results of individual methods for HPC fault case c (dotted lines refer to actual values)

in [14], is used. Faults in all individual components are included. Different types of faults are considered by involving one or more health parameters of a component.

A steady-state model of this engine is also employed [15] to simulate the measurements $\hat{\mathbf{y}}_k$ given:

1. set of command parameters $\mathbf{u}_k$
2. operating point $\hat{\mathbf{x}}_k$
3. health parameters $\hat{\mathbf{w}}_k$

Simulated measurements have been generated using the steady-state engine model during a cruise flight (ALT=10,800 m, M =0.82, DTAMB=0 K). Data sequences are generated with a duration of 5000 s with a data acquisition rate of 2 Hz. Profile of simulated faults is a steep fault with amplitude defined in Table 2 occurring at $t=50$ s followed by a slow drift of the same fault occurring at $t=2500$ s. In this way, the behavior of the method for both abrupt faults and gradual deteriorations is examined.

The time evolution of estimated health parameters will first be presented to show how the method traces their changes, abrupt or gradual. Representative test cases are chosen to demonstrate that the combined method performs better, not only when both constituents point to the same kind of answer, but also when the results of each method alone are different. Three such situations are chosen to be presented:

1. a fault on the high-pressure compressor (fault case c), which is solved by the Kalman filter, but not by the BBN
2. an LPT flow-capacity fault (case k), which is not solved by the Kalman filter but is solved by the BBN
3. an LPT fault involving two health parameters where none of the algorithms find the solution

HPC Fault: Case c. This case is dedicated to demonstrate the stability of the combination between the BBN and the Kalman filter. Both algorithms have been separately run on the same data set. The upper graph in Fig. 7 shows results of the diagnostic using the Kalman filter alone. It compares actual values of health parameter related to the high-pressure compressor (dotted lines) to identified values. Identified values are close to actual ones, showing that the identification is effective. No spreading of the fault is observed on the high-pressure turbine (not shown in the figure) nor on the fan and the low-pressure compressor. The lower graph in Fig. 7 shows similar results given by the BBN. Values in the ordinate of this graph are the corresponding mean computed by relation (5). As long as the fault is of small magnitude, namely, for

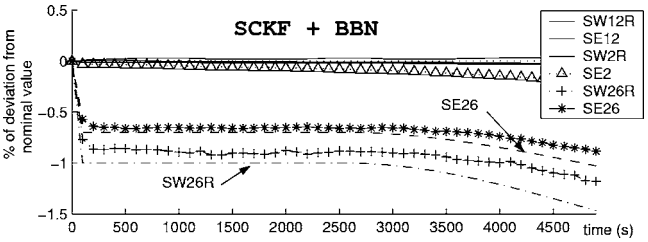

Fig. 8 Identification results of combined method for HPC fault case c (dotted lines refer to actual values)

~4000 s, the BBN produces a wrong diagnosis of an LPC fault (SE2). Only for the last period of the interval, when the deviation magnitude becomes larger, is the correct component indicated.

Results of the combined method are summarized in Fig. 8 showing that the fault is still correctly located by the Kalman filter. This demonstrates that the combined algorithm is not simply a weighted mean of Kalman filter and BBN results. It seems that the SCKF estimation is robust enough not to be perturbed by BBN information.

LPT Faults: Cases k and l. Test case k involves only one health parameter: the flow capacity of the low-pressure turbine (SW49R). This case is solved by the BBN but not by the Kalman filter. This situation is summarized in the upper graph in Fig. 9, which shows results for the turbine and the nozzle using the SCKF alone. Identified health parameters SW49R, SE49, as well as SE41 are detected faulty far from the actual values (dotted lines). Conversely, the BBN is able to locate the fault. The lower graph in Fig. 9 indicates that the parameter SW49R is low: mean values of SW49R are around −1%, which is close to the actual value. All other parameters are assigned to their nominal value indicating that the isolation is correct.

The following results (Fig. 10) highlight the benefit of the combination also for the BBN. Identified values related to SW49R are close to the actual one, whereas the one related to SE41 and SE49 remain close to nominal values. In this case the SCKF is driven by the BBN to the correct solution.

As another illustration of this, Fig. 11 shows the results of the test case l where both SW49R and SE49 are involved in the component fault. Values derived by the SCKF alone for SW49R and SE49 remain far from the actual ones, and the difference is spread on the other parameters (SW41R and SE41). The fault is correctly located, but its magnitude is not accurately determined. The combined algorithm identification is far more accurate. The fault is not only located correctly but also accurately assessed.

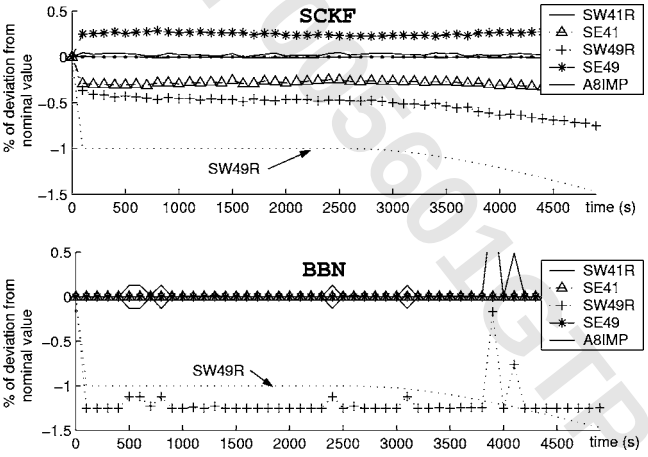

Fig. 9 Identification results of individual methods for LPT fault case k (dotted lines refer to actual values)

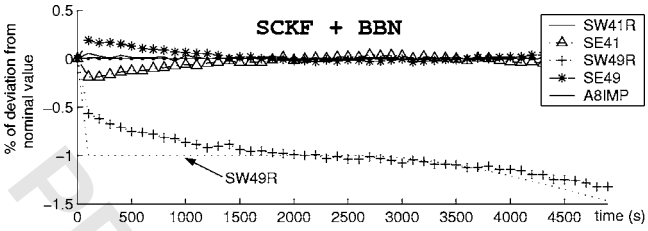

Fig. 10 Identification results of combined method for LPT fault case k (dotted lines refer to actual values)

LPT Fault: Case j. Because no interturbine measurement is available, case j is by far the most difficult one. This case is not solved by the BBN nor the SCKF, which is represented in Fig. 12 where values of SW49R, SE49, and SE41 identified by the SCKF remain far from actual values. Therefore, both low- and high-pressure turbines are detected as faulty. The same kind of results are obtained using the BBN where SW49R and SW41R are classified as faulty, while the fault related to SE49 is not detected.

Although identified values of SW49R and SE49 are closer to the actual ones, the fault remains poorly located (Fig. 13). SE41 is below −0.3%, and the high-pressure turbine also looks defective.

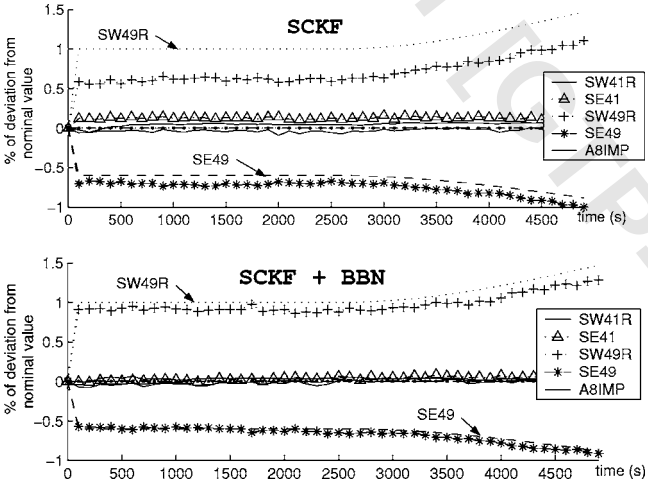

Fig. 11 Identification results of SCKF (upper figure) and combined method (lower figure) for LPT fault case l (dotted lines refer to actual values of health parameters)

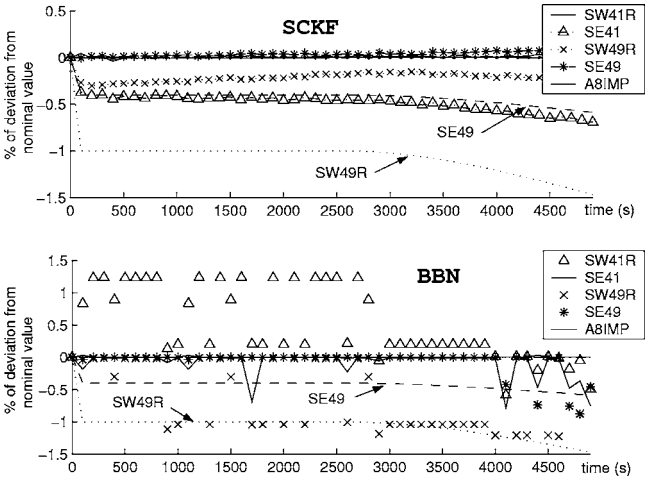

Fig. 12 Identification results of individual methods for LPT fault case j (dotted lines refer to actual values)

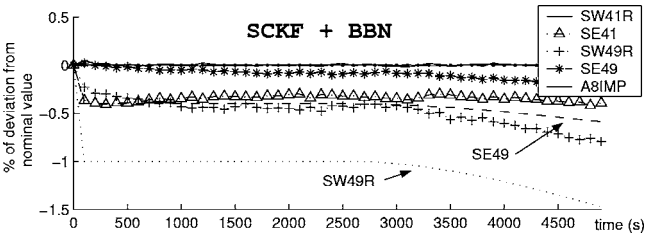

Fig. 13 Identification results of combined method for LPT fault case j (dotted lines refer to actual values)

This behavior is not surprising since not one of the constituent methods provides information that could be used to lead the combined method to the correct decision.

Diagnostic Effectiveness Overview. In order to illustrate the capabilities of the method, application results related to a number of different fault cases are shown. Table 3 compares the results of the soft-constrained Kalman filter (SCKF) alone to the combination of the SCKF with the BBN. This table shows maximum absolute value of biases $\Delta \mathbf{w}_k$ achieved by both methods after 4900 measurement samples are observed, which represents an image of the asymptotic efficiency of the method.

$$\Delta \mathbf{w}_k = 100 \frac{\hat{\mathbf{w}}_k - \mathbf{w}_k^{actual}}{\mathbf{w}_k^{nominal}} \tag{7}$$

Values of $\Delta \mathbf{w}_k$ around 0.25% are considered acceptable. The main conclusion of these results is that the combination especially improves results of the Kalman filter in test cases j, k, and l related to the low-pressure turbine.

Table 4 gives an overall picture of the efficiency and the gain achieved by the combination is compared to SCKF and BBN working separately. This combination is able to solve all the test cases except the case j, which is known to be difficult to identify with this set of seven measurements [7].

Discussion

The present recursive method allows one to identify component faults based on associated measurement deviations whose amplitude is around the standard deviation of measurement noise. The signal-to-noise ratio mainly affects the identification process in terms of convergence speed. The dependency of the convergence speed on the measurement noise level is illustrated in Fig. 14. Crosses represent the relative increase of time required to accumulate enough data samples as needed to converge to the asymptotic solution. The crosses compare well to the theoretical

Table 3 Comparison of identification results using soft-constrained Kalman filter with noninformative a priori (left column) and BBN a priori (right column). Results are maximum absolute values of biases defined by (7)

	SCKF alone (%)	SCKF+BBN(%)
a	0.03 on SW49R	0.05 on SW49R
b	0.09 on SE12	0.10 on SE12
c	0.07 on SW26R	0.12 on SW26R
d	0.03 on SE12	0.06 on SE2
e	0.03 on SW26R	0.04 on SW49R
f	0.02 on SE42	0.02 on SE42
g	0.17 on SW49R	0.11 on SE49
h	0.24 on SW49R	0.14 on SW49R
i	0.19 on SW49R	0.25 on SW49R
j	0.82 on SW49R	0.58 on SW49R
k	0.53 on SW49R	0.04 on SW49R
l	0.41 on SW49R	0.12 on SW49R
m	0.06 on SE41	0.05 on SE41
n	0.06 on SW2R	0.03 on SE49

PROOF COPY [GTP-04-1071] 005601GTP

Table 4 Summary of diagnosis success given by the SCKF alone, BBN alone, and combination of the SCKF with BBN a priori for the complete set of component fault detailed in Table 2

	SCKF	BBN	SCKF+BBN
a	√	√	√
b	√	√	√
c	√	-	√
d	√	√	√
e	√	√	√
f	√	√	√
g	√	√	√
h	√	√	√
i	√	√	√
j	-	-	-
k	-	-	-
l	-	√	-
m	√	√	√
n	√	√	√

prediction (plain line), which states that the number of data samples required to obtain a given accuracy must increase as a quadratic function of the noise level. Indeed, more accurate measurements (less noise) means more adaptability (since the Kalman gain **K** is higher), an improved tracking capability, and, therefore, an increased convergence speed.

Moreover, systematic calculations have shown that the final diagnostic (asymptotic solution) is only slightly affected by the level of noise in the measurements. Beside these effects of the noise level, the nonobservability of some parameters can lead to a false diagnostic even though the noise level is strongly reduced.

With the set of seven available measurements, those results are the most meaningful that can be obtained with the combined algorithm. In order to obtain a better location of the fault, additional knowledge must be made available. In [8], two additional measurements are considered: P26 and P49. Although this solution is ideal because it provides the best results, those two measurements may not be available. In a test bench configuration it may happen that some other measurements are available (i.e., vibrations, some measurements about the lubrication system, etc.) but are unlikely to be predicted based on the health parameters since they do not appear in the model. This underlines the weakness of the Kalman filter for which a model has to be available. Any qualitative knowledge is very difficult to include in the identification procedure.

The combined method proposed in the present paper allows the inclusion of additional information from sources other than modeled measurements (information fusion). It can thus produce results that would have been possible for the Kalman filter only with additional gas path measurements. This point is demonstrated by considering again case j, but assuming now that some additional information exists, such as historical records and related statistics.

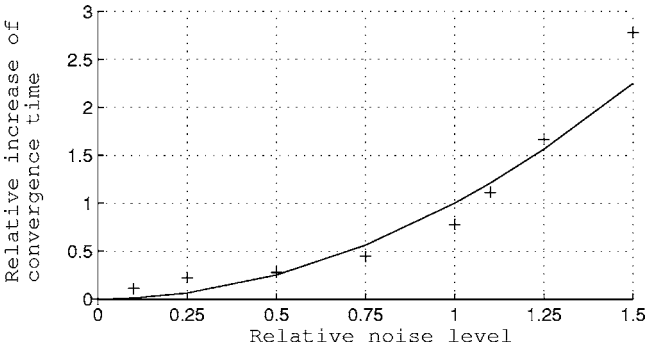

Fig. 14 Influence of the measurement noise level on the convergence speed

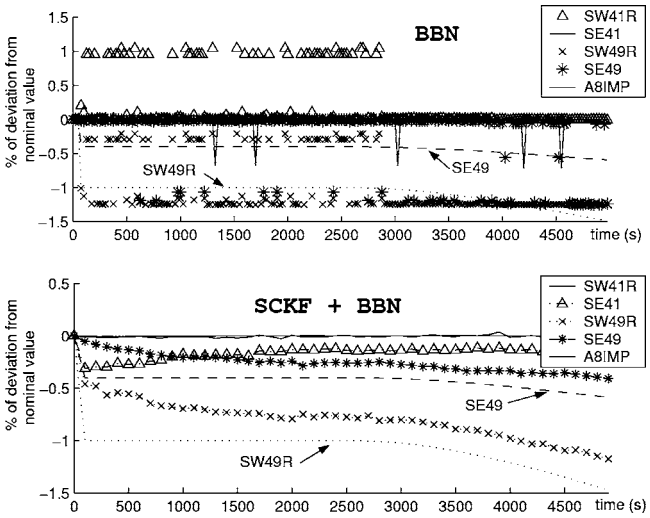

Fig. 15 Identification results of BBN alone (upper figure) and combined method (lower figure) for LPT fault case j (dotted lines refer to actual values)

The following test case assumes that such additional knowledge favors a fault on the low-pressure turbine. The BBN is modified by tuning the a priori knowledge about the health parameters (see [9] for the detailed procedure) to make a fault on the low-pressure turbine more likely to occur.

Results using this "modified" BBN are shown in Fig. 15. A fault on SE49 is now detected in addition to the one related to SW49R. Results of the combined algorithm (lower graph in Fig. 15) are far better: SW49R as well as SE49 converge to their actual value, while SE41 is closer to its true value. Finally (after 2500 s), the detection is effective and the health parameters are accurately assessed. The diagnosis is effective and allows a more reliable decision.

Conclusions

A new methodology combining classification methods and regression methods has been developed in order to benefit of their mutual advantages. This combination has been tested on cases representative of a real-life application to underline the gain in stability and accuracy that can be achieved. The number of undetected faults are lowered and false alarms are avoided (Table 4) when compared to regression or classification methods working separately.

The estimation of the combined algorithm allows a more reliable detection of component faults but also achieves a better accuracy and a better fault isolation by lowering the spread of the fault on several parameters ("smearing effect").

Besides the improvements in accuracy and stability, this kind of method allows information or sensor fusion, which is a very important field of research for future works. The key advantage of combining methods is that it replaces the problem of comparing classification techniques to regression techniques by the problem of choosing which information they can share.

Acknowledgments

The paper has been produced in the framework of a collaboration between the ASMA Department of the University of Liege (Belgium) and the Thermal Turbomachinery Laboratory (LTT) of the National Technical University of Athens (Greece). This work is funded by the Walloon Region of Belgium in its Program FIRST and supported by Techspace Aero, Snecma Group.

Nomenclature

BBN = Bayesian Belief Network

$\mathbf{D}$ = covariance matrix of $\mathbf{w}_{\text{prior}}$
$\mathcal{G}$ = nonlinear engine performance model
k = time index (discrete time)
KF = Kalman filter
$\bar{\mathbf{r}}_k$ = residuals on raw measurements $\bar{\mathbf{r}}_k = \bar{\mathbf{y}}_k - \hat{\mathbf{y}}_k$
$\mathbf{R}_r$ = covariance matrix of $\bar{\mathbf{r}}_k$
$\mathbf{R}_y$ = covariance matrix of $\bar{\mathbf{y}}_k$
SCKF = soft-constrained Kalman filter
t = time
$\mathbf{u}_k$ = command parameters
$\mathbf{w}_k$ = engine health parameters
$\mathbf{w}_{\text{prior}}$ = a priori value of health parameters
$\hat{\mathbf{w}}_k$ = estimated engine health parameters
$\mathbf{x}_k$ = engine operating point
$\hat{\mathbf{x}}_k$ = estimated engine operating point
$\mathbf{y}_k$ = measurements involved in health parameter estimation
$\bar{\mathbf{y}}_k$ = raw measurements $\mathbf{y}_k$ from data acquisition system
$\hat{\mathbf{y}}_k$ = estimation of measurements $\mathbf{y}_k$
$\mathbf{z}_k$ = measurements involved in operating point estimation
$\bar{\mathbf{z}}_k$ = raw measurements $\mathbf{z}_k$ from data acquisition system

References

[1] Bishop, C. M. 1995, *Neural Networks for Pattern Recognition*, Clarendon Press, Oxford.
[2] Volponi, A., 2003, "Foundation of Gas Path Analysis (Part i and ii)," *Von Karman Institute Lecture Series: Gas Turbine Condition Monitoring and Fault Diagnosis, (2003-01)*.
[3] Provost, M. J., 2003, "Kalman Filtering Applied to Gas Turbine Analysis," *Von Karman Institute Lecture Series: Gas Turbine Condition Monitoring and Fault Diagnosis, (2003-01)*.
[4] Kobayashi, T., and Simon, D. L., 2003, "Application of a Bank of Kalman Filters for Aircraft Engine Fault Diagnostics," *ASME Turbo Expo*, ASME Paper No. GT2003-38550.
[5] Aretakis, N., Mathioudakis, K., and Stamatis, A., 2002, "Non-linear Engine Component Fault Diagnosis From a Limited Number of Measurements Using a Combinatorial Approach," *ASME Turbo Expo*, ASME Paper No. GT2002-30031.
[6] Simon, D., and Simon, D. L., 2003, "Aircraft Turbofan Engine Health Estimation Using Constrained Kalman Filtering," *ASME Turbo Expo*, ASME Paper No. GT2003-38584.
[7] Grodent, M., and Navez, A., 2001, "Engine Physical Diagnosis Using a Robust Parameter Estimation Method," *37th AIAA/ASME/SAE/ASEE Joint Propulsion Conference*.
[8] Dewallef, P., Mathioudakis, K., and Léonard, O., 2004, "On-Line Aircraft Engine Diagnostic Using a Soft-Constrained Kalman Filter," *ASME Turbo Expo*, ASME Paper No. GT2004-53539.
[9] Romessis, C., and Mathioudakis, K., 2004, "Bayesian Network Approach for Gas Path Fault Diagnosis," *ASME Turbo Expo*, ASME Paper No. GT2004-53801.
[10] Mathioudakis, K., 2003, "Neural Networks in Gas Turbine Fault Diagnosis," *Von Karman Institute Lecture Series: Gas Turbine Condition Monitoring and Fault Diagnosis, (2003-01)*.
[11] Brotherton, T., Volponi, A., Luppold, R., and Simon, D. L., 2003, "Estorm: Enhanced Selft Tuning On-Board Real-Time Engine Model," *2003 IEEE Aerospace Conf.*
[12] Moody, J. E., 1992, "The Effective Number of Parameters: An Analysis of Generalization and Regularization in Nonlinear Learning Systems," *Advances in Neural Information Processing System 4*, ■, ■.
[13] MacKay, D. J. C., 1995, "Bayesian Methods for Neural Networks: Theory and Application," Tech. Report, Cavendish Laboratory, University of Cambridge, http://wol.ra.phy.cam.ac.uk
[14] Curnock, B., 2000, Obidicote Project-Word Package 4: Steady-State Test Cases, Tech. Report DNS62433, Rolls-Royce.
[15] Stamatis, A., Mathioudakis, K., Ruiz, J., and Curnock, B., 2001, "Real-Time Engine Model Implementation for Adaptive Control and Performance Monitoring of Large Civil Turbofans," *ASME Turbo Expo*, ASME Paper No. GT2001-362.

PROOF COPY [GTP-04-1071] 005601GTP